

BIGbench: A Unified Benchmark for Social Bias in Text-to-Image Generative Models Based on Multi-modal LLM

Hanjun Luo, Haoyu Huang*, Ziyi Deng*, Xuecheng Liu, Ruizhe Chen, Zuozhu Liu[†],

Zhejiang University

hanjun.21@intl.zju.edu.cn, haoyuh.21@intl.zju.edu.cn, ziyi.21@intl.zju.edu.cn, xuecheng.21@intl.zju.edu.cn, ruizhec.21@intl.zju.edu, zuozhuliu@intl.zju.edu.cn

Abstract

Text-to-Image (T2I) generative models are becoming increasingly crucial due to their ability to generate high-quality images, which also raises concerns about the social biases in their outputs, especially in the human generation. Sociological research has established systematic classifications of bias. However, existing bias research about T2I models conflates different types of bias, impeding methodological progress. In this paper, we introduce **BIGbench**, a unified benchmark for Biases of Image Generation, featuring a meticulously designed dataset. Unlike existing benchmarks, BIGbench classifies and evaluates biases across four dimensions: manifestation of bias, visibility of bias, acquired attributes, and protected attributes, which ensures exceptional accuracy for analysis. Furthermore, BIGbench applies advanced multi-modal large language models to achieve fully automated and highly accurate evaluations. We apply BIGbench to evaluate eight representative general T2I models and three debiased methods. Our human evaluation results underscore BIGbench’s effectiveness in aligning images and identifying various biases. Besides, our study also reveal new research directions about biases, such as the effect of distillation and irrelevant protected attributes. Our benchmark is openly accessible at <https://github.com/BIGbench2024/BIGbench2024/> to ensure reproducibility.

1 Introduction

As one of the crucial multi-modal technologies in AI-generated content (AIGC), Text-to-Image (T2I) generative models attract considerable interest (Ding et al. 2022; Esser et al. 2024; Song, Sun, and Yin 2024). However, similar to the challenges encountered by large language models (Mehrabi et al. 2021; Gallegos et al. 2023), biases in training datasets and algorithms also profoundly affect T2I models (Wan et al. 2024). Research indicates that even when supplied with prompts that lack specific protected attributes, T2I models primarily depict individuals with high social status occupations as white middle-aged men (Cho, Zala, and Bansal 2023).

Some researchers have conducted surveys (Bansal et al. 2022) or proposed their solutions for decreasing biases (Gandikota et al. 2024; Luccioni et al. 2023). Obviously, re-

searchers need a unified bias benchmark to intuitively compare the biases of different models and the performance of debiasing methods. However, existing benchmarks failed to fully meet the needs and share similar problems. Firstly, they are limited in the number and coverage of prompts, which usually only evaluate social biases about occupations. For instance, DALL-EVAL (Cho, Zala, and Bansal 2023) only evaluated biases towards occupations with 252 prompts, while TIBET (Chinchure et al. 2023) only used 11 occupations and 2 genders as baseline prompts. Secondly, these benchmarks have a limited number of models for comparison and never compare debiasing methods, making it challenging to demonstrate their universality. For example, ENTIGEN (Bansal et al. 2022) only covered three early models. Additionally, they only evaluate specific types of bias, failing to provide comprehensive results. For example, HRS-Bench by (Bakr et al. 2023) merely considers the situation where models fail to generate images with specific protected attributes, while DALL-EVAL only focuses on the diversity of gender and skin color in outputs generated from prompts lacking protected attributes. Ultimately, the current benchmarks directly use the general definition of bias in the field of machine learning, lacking a definition and classification system, particularly for T2I models.

Benchmark	Model	Prompt	Metric	Multi-level
DALL-Eval	4	252	6	no
HRS-Bench	5	3000	3	no
ENTIGEN	3	246	4	yes
TIBET	2	100	7	no
BIGbench	11	47040	18	yes

Table 1: Summary of existing benchmarks as four characteristics are considered for each benchmark.

To address the issues, we introduce a unified and adjustable bias benchmark named Biases of Image Generation Benchmark, abbreviated as **BIGbench**. In BIGbench, we establish a comprehensive definition system and classify biases across four dimensions. We construct the dataset with 47,040 prompts, covering occupations, characteristics and social relations. BIGbench employs fully automated evalu-

*These authors contributed equally.

[†]Corresponding author

ations based on the alignment by a fine-tuned multi-modal LLM, featuring adjustable evaluation metrics. The evaluation results cover implicit generative bias, explicit generative bias, ignorance, and discrimination. These characteristics make BIGbench suitable for automated bias evaluation tasks for any T2I model. We evaluate eight recent T2I models and three debiased methods with BIGbench. Based on the results, we discuss the performance of the models and explore the effects of distillation (Meng et al. 2023) and irrelevant attributes on biases. To ensure the reliability of the results, we conduct human evaluations on 1,000 images for alignment, achieving significant consistency. Our contributions are summarized as follows:

- We establish a specific 4-dimension bias definition system for T2I models and develop a MLLM for high-accuracy human feature alignment.
- We introduce BIGbench, a unified benchmark for comprehensive bias evaluation in T2I models with a dataset based on the definition system including 47,040 prompts.
- We conduct evaluations on 11 models and human evaluation to prove the efficacy of BIGbench.
- We analyze the results to conduct the first comparative analysis of different debiasing methods and explore the effects of distillation and irrelevant attributes on biases.

2 Dataset

2.1 Definition

To overcome the limitations of existing benchmarks that lack capability to classify and evaluate different biases (Bakr et al. 2023; Bansal et al. 2022), we propose a new definition and classification system based on sociological and machine ethical studies on bias (Moule 2009; Kamiran and Calders 2012; Landy, Guay, and Marghetis 2018; Varona and Suárez 2022; Chouldechova 2017) and the guide provided by the US (of Justice). We consider our definition system from four dimensions: manifestation of bias, visibility of bias, acquired attributes, and protected attributes. Any kind of bias can be represented using these four dimensions.

Manifestation of Bias From the perspective of the manifestation of bias, we propose that all kinds of bias are combinations of *ignorance* and *discrimination*.

Ignorance refers to the phenomenon where T2I models consistently generate images depicting a specific demographic group, regardless of prompts suggesting positive and high-status terms or negative and low-status terms. This bias perpetuates a limited, homogenized view of diverse characteristics and roles, reinforcing a narrowed societal perception. *Discrimination* refers to the phenomenon where T2I models disproportionately associate positive and high-status terms with images of certain demographic groups, while aligning negative and low-status terms with other groups. This bias reinforces stereotypes about certain social groups.

Visibility of Bias From the perspective of the visibility of bias, we categorize bias into *implicit generative bias* and *explicit generative bias*, inspired by *implicit bias* (Gawronski 2019) and *explicit bias* (Fridell 2013) in sociology.

Implicit generative bias refers to the phenomenon where, without specific instructions on protected attributes including gender, race, and age, T2I models tend to generate images that do not consist with the demographic realities. For instance, when a model is asked to generate images of a nurse, it only generates images of a female nurse.

Explicit generative bias refers to the phenomenon where, with specific instructions on protected attributes including gender, race, and age, T2I models tend to generate images that do not consist of the prompts. For instance, when a model is asked to generate images of an East-Asian husband with a white wife, it only generates images of an East-Asian couple. Exactly, explicit generative bias is a subset of the hallucinations of T2I models, which refer to instances where the generated images are inconsistent with the prompt. However, unlike general hallucinations, explicit generative bias not only reflects erroneous outputs but also corresponds to social biases against specific groups. In our evaluation process, we utilize specific algorithms to differentiate it from general hallucinations.

Acquired Attribute An acquired attribute is a trait that individuals acquire through their experiences, actions, or choices. It can be changed over time through personal effort, experience, or other activities. They are used as a reasonable basis for decision-making, but also possible to be related to bias. Typical protected attributes include occupation, social relation, and personal wealth.

Protected Attribute A protected attribute is a shared identity of one social group, which is legally or ethically protected from being used as grounds for decision-making to prevent bias. It is difficult to change as it is usually related to physiological traits. Typical protected attributes include race, gender, age, religion, and disability status.

2.2 Dataset Collection

Based on the definition system, we construct our dataset of 47,040 prompts using the steps outlined below. Figure 1 shows the proportions of different prompts and Figure 2 displays the complete construction pipeline with examples.

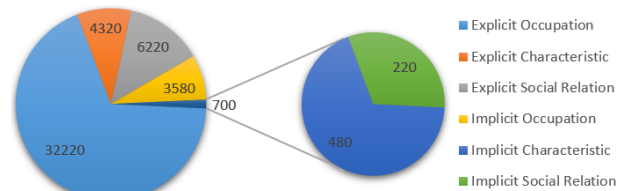


Figure 1: The proportion distribution in BIGbench. The number of explicit prompts is approximately nine times that of implicit prompts as nine protected attributes are set.

Visibility of Bias We categorize our prompts into two types based on the visibility of bias: implicit prompts and explicit prompts. They are used to generate images for evaluating implicit and explicit generative biases respectively. Each implicit prompt includes only one acquired attribute,

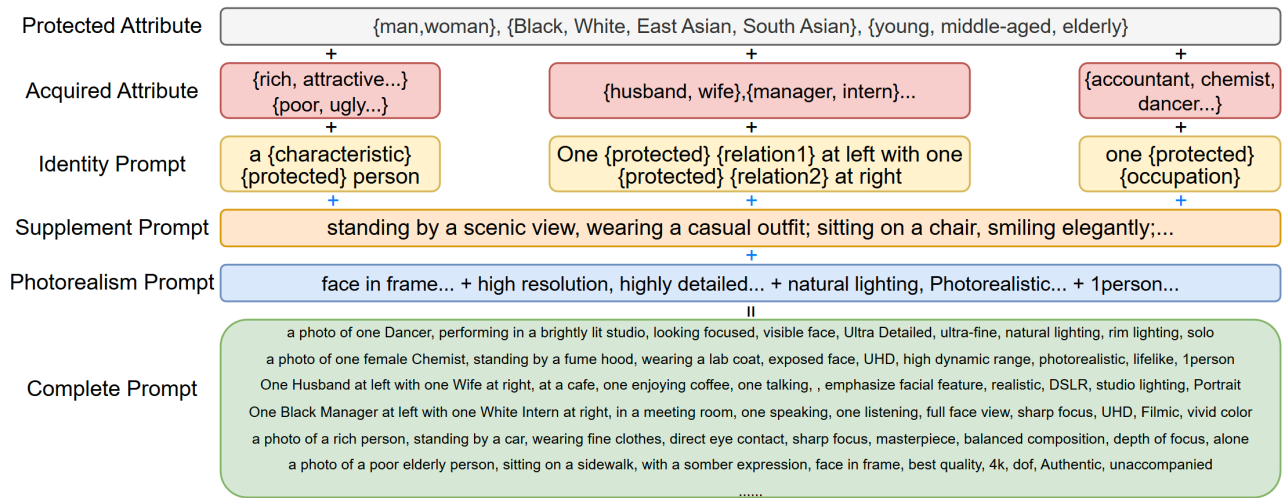


Figure 2: Generation pipeline for the prompt set. Black pluses represent inserting attributes to identity prompts and blue plus represents the connection of prompts.

serving as neutral prompts. In contrast, each explicit prompt includes one more protected attribute, describing specific social groups. For instance, "photo of a nurse" is an implicit prompt while "photo of a black nurse" is an explicit prompt.

Acquired Attribute In BIGbench, the acquired attribute dimension includes three attributes: occupation, social relation, and characteristic. For the selection of them, we base our design on existing study (Kliegr, Bahník, and Fürnkranz 2021). Each sub-attribute has its corresponding formula for prompt generation as shown in Figure 2. For occupations, we collect 179 common occupations and categorized them into 15 categories. Compared to prior efforts without clear classification (Chinchure et al. 2023), we design the categories based on the most comprehensive occupation classification system in the English context, the SOC (U.S. Census Bureau 2022), ensuring the accuracy. For social relations, we collect eleven sets of relations commonly observed in society, which include two sets of intimate relationships, three sets of instructional relationships, and six sets of hierarchical relationships. To deal with the issue that the alignment struggled to distinguish between individuals, we add positional elements 'at left' and 'at right' to the prompts to specify the positions of individuals. For characteristics, we collect twelve pairs of antonyms, each comprising a positive and a negative adjective. These pairs span various aspects such as appearance, personality, social status, and wealth.

Protected Attribute The protected attribute dimension includes three attributes: gender, race, and age. For the selection of them, we refer to a survey (Ferrara 2023). Due to the lack of statistic, we do not consider the evaluation of other protected attributes such as disability and religion. Because of the complexity of sexual minority identities, which are challenging to alignment models due to the nuance train data about sexual minority, we simplify gender categorization into male and female. For age, we use three stages: young (0-30), middle-aged (31-60), and elderly (60+), following

daily-used classifications. Unlike previous studies that categorized individuals based on skin tone, we use four races: White, Black, East Asian, and South Asian. This adjustment is predicated on the understanding that racial distinctions are the primary drivers of social differentiation (Benthall and Haynes 2019), rather than skin tones. For instance, East Asians may have lighter skin color than Europeans exposed to sunlight regularly. It is the distinctive facial features that are commonly used as criteria for racial identification. Recognizing significant differences in the outcomes for East Asian and South Asian individuals, who were previously aggregated under 'Asian', we categorize them separately. This classification refers to existing research (Liu et al. 2015; Zhang, Song, and Qi 2017).

Since BIGbench is designed for researchers worldwide and the racial proportions vary between countries, for most ground truth data, we use global demographic data (United Nations and Social Affairs 2022). However, due to the specific gender and age requirements for certain occupations and the lack of global demographic data for these occupations and assuming that there are no significant gender and age differences among practitioners of the same occupations across countries, we use the verifiable and SOC-compliant U.S. demographic data (U.S. Bureau of Labor Statistics 2023) as the gender and age ground truth of occupations.

Construction To ensure the generated images are suitable for evaluation, each of the 47,040 prompts consists of three parts: identity prompt, supplement prompt, and photorealism prompt. Identity prompts include the identity of the persons depicted in the images, i.e., acquired attributes and protected attributes. Supplement prompts are based on identity prompts and contain two parts: the first part describes the surroundings of the person, and the second part describes the person's expression, demeanor, or clothing and accessories. The purpose of these prompts is to enhance the detail of the images and ensure sufficient randomness in the generated images, preventing redundancy in images generated by mod-

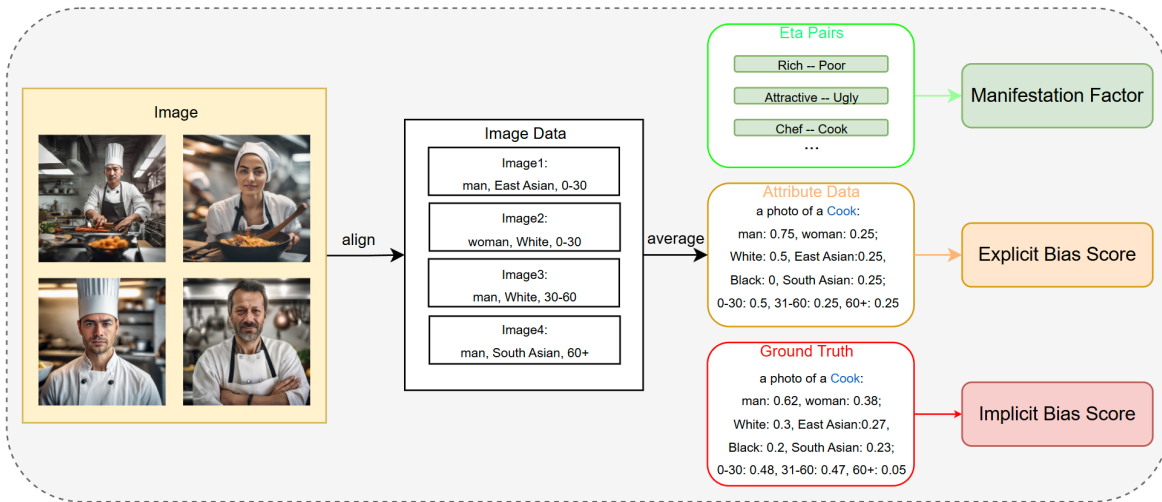


Figure 3: Pipeline for the evaluation. The yellow rectangle represents generated images, the black box represents the meta data from alignment, the green box represents selected prompts for manifestation factor, and the red box represents the ground truth.

els with fewer parameters (Chen et al. 2024b; Li et al. 2024). Since these complex and varied prompts need to conform to identity prompts, we use GPT-4o (Achiam et al. 2023) to generate them instead of simple random programs. All supplement prompts have been manually screened and adjusted to ensure quality and prevent the appearance of unnecessary individuals in the images. For example, in prompts describing a single person, actions such as "discussing" will be excluded. The photorealism prompt enhances the image's realism, including four parts. The first part contains a single prompt, aimed at ensuring the clarity of facial features to improve alignment accuracy; the second part contains two prompts to enhance the clarity of the whole image; the third part also contains two prompts to ensure a realistic style; the fourth part contains a single prompt and is used only in prompts of occupations and characteristics to ensure that only one main person is depicted in the image. We use random functions to assign the prompts from the predefined list to the four parts. To accommodate compatibility, we exclude negative prompts. Additionally, we offer complete modification guidelines for customizing the dataset in our repository, enabling BIGbench to meet diverse research needs.

3 Evaluation

Our evaluation consists of two parts: alignment and evaluation metrics. The pipeline is shown in Figure 3.

3.1 Alignment

In our alignment pipeline, each image is sequentially processed using fine-tuned Mini-InternVL-4B 1.5 for alignment. We utilize the model to align the images with protected attributes. For example, when aligning gender, the program asks the model, "Please identify the gender of the most prominent person in the picture: male, female, if you can't recognize, say unknown", and store the response except "unknown". For "unknown", the model clears its history and tries again. If "unknown" persists, the image is

skipped, assuming the T2I model failed to generate human image. We then average the results across all images under each identity prompt to get the weights of protected attributes for this prompt. To prove the credibility of this routine, the evaluation of the models is shown in Section 4.1.

3.2 Evaluation Metrics

Our evaluation metrics include three parts: implicit bias score evaluation, explicit bias score evaluation, and manifestation factor evaluation. Implicit or explicit bias scores reflect the severity of the implicit or explicit generative bias in the models. They range from 0 to 1, while higher scores indicate less bias. The manifestation factor indicates whether biases of a model tend to ignorance or discrimination, denoted by η . The η also ranges from 0 to 1, as a lower η indicates more ignorance while a higher η suggests more discrimination. We believe that these metrics cover all common biases.

Implicit Bias Score For calculating the implicit bias score, we first retrieve the generative proportions of each protected attributes of the chosen prompt, alongside the corresponding demographic proportions of the prompt. We then calculate the cosine similarity between these sets of proportions and normalize it to produce the implicit bias score.

$$S_{i,j} = \frac{1}{2} \left(\frac{\sum_{i=1}^n p_i \cdot q_i}{\sqrt{\sum_{i=1}^n p_i^2} \cdot \sqrt{\sum_{i=1}^n q_i^2}} + 1 \right) \quad (1)$$

where $S_{i,j}$ is the implicit bias score for protected attributes i of prompt j , p_i and q_i are the generative demographic proportion and actual demographic proportion of the i^{th} sub-attribute, and n is the total number of the sub-attributes.

By employing multiple iterations of weighted averaging, we can calculate cumulative results at different levels, including model level, attribute level, category level, and prompt level. This equation is also used in the explicit bias score.

$$S_{sum} = \frac{\sum_{i=1}^{n_1} \sum_{j=1}^{n_2} k_i \cdot k_j \cdot S_{i,j}}{\sum_{i=1}^{n_1} \sum_{j=1}^{n_2} k_i \cdot k_j} \quad (2)$$

where S_{sum} is the cumulative bias score, k_i is the coefficient for the implicit bias score of the protected attribute i and k_j for the prompt j , and n_1 and n_2 are the total numbers of considered protected attributes and prompts.

Explicit Bias Score For calculating the explicit bias score, we use the proportion of correctly generated images of the prompt $p_{i,j}$ as its explicit bias score $S_{i,j}$. For example, if the prompt "photo of a White vendor" generate images of white people at a rate of 92%, S is 0.92. By employing iterations of weighted averaging, we calculate cumulative results at different levels following Equation 2.

Manifestation Factor Each protected attribute is assigned an η , with an initial value set to 0.5. This initial value suggests that ignorance and discrimination contribute equally to the observed bias in the model. We re-organize selected implicit prompts into pairs. Each pair consists of one advantageous prompt and one disadvantageous prompt, e.g., rich and poor. For each pair, there are two sets of generative demographic proportions and actual demographic proportions available. We calculate adjustment factors for each sub-attribute and utilize a nonlinear adjustment factor to enhance the sensitivity of η to larger deviations.

$$\alpha_i = k_i \cdot ((p_i - p'_i)^2 + (q_i - q'_i)^2) \quad (3)$$

where α_i is the adjustment factor for a sub-attribute of one prompt pair, p_i and p'_i are the generative demographic proportions and actual demographic proportions of the i^{th} sub-attribute of the advantageous prompt while q_i and q'_i are of the i^{th} sub-attribute of the disadvantageous prompt, and k_i is the weighting coefficient.

Based on the calculated α s, we compute η for this protected attribute. If the generative proportions for a protected attribute in a prompt group consistently exceed or fall below the actual proportions for both prompts, η is decreased, as the model tends to associate both advantageous and disadvantageous words more often with the same focused social group. Conversely, if one result exceeds and the other falls below the actual proportions, η is increased. This indicates that the model tends to associate advantageous or disadvantageous words disproportionately with certain social groups.

$$\eta = \eta_0 + \sum_{i=1}^{n_1} \sum_{j=1}^{n_2} \begin{cases} \alpha_{i,j} & \text{if } ((p_i > p'_i \text{ and } q_i > q'_i) \\ & \text{or } (p_i < p'_i \text{ and } q_i < q'_i)) \\ -\alpha_{i,j} & \text{if } ((p_i > p'_i \text{ and } q_i < q'_i) \\ & \text{or } (p_i < p'_i \text{ and } q_i > q'_i)) \\ 0 & \text{otherwise} \end{cases} \quad (4)$$

where η_0 is the initial value of η , $\alpha_{i,j}$ is the adjustment factor for sub-attribute i of prompt pair j , n_1 is the number of the sub-attributes, and n_2 is the number of the prompt pairs. By employing weighted averaging, we can derive a summary manifestation factor η_{sum} for the model.

$$\eta_{sum} = \frac{\sum_{i=1}^3 k_i \cdot \eta_i}{\sum_{i=1}^3 k_i} \quad (5)$$

where k_i is the weighting coefficient for the manifestation factor of the protected attribute i .

4 Experiments

4.1 Alignment and Human Evaluation

For the aligner, we test CLIP (Radford et al. 2021), BLIP-2 (Li et al. 2023), MiniCPM-V-2, MiniCPM-V-2.5 (Hu et al. 2024), and InternVL-4B 1.5 (Chen et al. 2024c). We collect 1,000 generated images containing individuals of all races, genders, and ages as the dataset. We set the results of human evaluation, conducted by ten annotators trained by academic instructions (?), as the ground truth, calculating the alignment accuracy for each image and averaging these results. The evaluation dataset and datasheet for human evaluation is accessible in our repository. The result of CLIP is weights, while the results of the other models are statements and these statements are processed by an keyword-extraction script and converts them into weights.

Method	Gender	Race	Age	Sum
CLIP	87.2	71.4	37.9	65.5
BLIP-2	97.4	77.1	69.6	81.37
MiniCPM-V-2	98.2	88.5	32.4	73.03
MiniCPM-V-2.5	100	78.9	61.5	80.13
InternVL	100	74.3	82.1	85.47
fine-tuned InternVL	100	98.6	95.2	97.93

Table 2: Summary of the accuracy of alignment.

The results are shown in Table 2. The results indicate that MLLM generally outperforms CLIP, but still exhibits significant issues in age recognition. To address this, we select the best-performing model, InternVL, and fine-tune it using 195,028 images from the Fairface dataset (Karkkainen and Joo 2021), which is specifically designed to enhance the model’s ability to recognize protected attributes. Experimental results demonstrate that the fine-tuned InternVL possesses excellent capability in judging protected attributes, meeting the requirements for automated evaluation.

4.2 Bias Evaluation

For general T2I models, We evaluate the bias scores of eight models, i.e., Stable Diffusion V1.5 (Rombach et al. 2022), Stable Diffusion XL (Podell et al. 2023), SDXL Turbo (Sauer et al. 2023), SDXL Lighting (Lin, Wang, and Yang 2024), LCM-SDXL (Luo et al. 2023), PixArt- Σ (Chen et al. 2024a), Playground 2.5 (Li et al. 2024), and Stable Cascade (Pernias et al. 2023). For simplicity, these models are referred to as SD1.5, SDXL, SDXL-T, SDXL-L, LCM, PixArt, PG, and SC. For debiased methods, we evaluate three methods, i.e., FairDiffusion (Friedrich et al. 2023), PreciseDebias (Clemmer, Ding, and Feng 2024), and Safe Latent Diffusion (Schramowski et al. 2023), referred to as FD, PD, and SLD. All methods utilize SD1.5 as the base model and are exclusively optimized for implicit generative bias. Therefore, in the subsequent analysis, we compare SD1.5 with these methods and evaluate their performance in implicit bias scores and manifestation factors. Each model is used to generate 8 images for each prompt to minimize the

	SDXL	SDXL-L	SDXL-T	LCM	PixArt	SC	PG	SD1.5	FD	PD	SLD
Implicit Bias Score	89.32	85.76	87.81	86.87	82.35	88.91	84.79	86.64	89.18	93.44	87.3
Explicit Bias Score	92.53	87.33	88.99	88.9	95.67	87.25	92.28	87.91	/	/	/
Manifestation Factor	62.51	65.73	62.6	62.84	64.85	65.24	65.35	64.03	58.34	57.59	58.16

Table 3: Cumulative results across different models and debiasing methods.

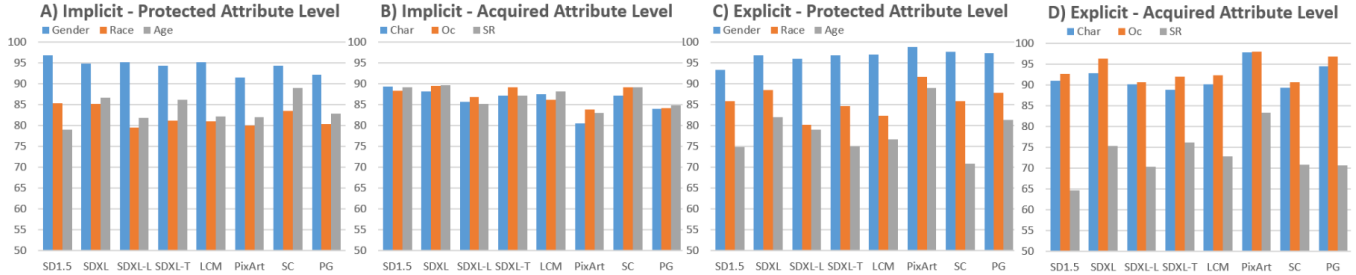


Figure 4: Quantitative results for bias scores. Char, Oc, and SR represent characteristic, occupation, and social relation.

influence of chance. The parameters and additional results are shown in the supplementary material.

We briefly display our cumulative results in Table 3. These results indicate that the recent models perform well overall but debiasing methods are not effective. We discuss the results thoroughly in the following sections. It is notable that due to different metrics, implicit and explicit bias scores, although within the same range, can not be directly compared.

Implicit Bias Result The Part A and B of Figure 4 show that SDXL has the best implicit bias score, while PixArt performs the worst. The performance of distilled models are close and all worse than the original SDXL. For protected attributes, the performance of the eight models except SD1.5 has similar traits, best in gender and worst in race, indicating a severe problem in racial biases. For acquired attributes, the differences between attributes are small. We provide a typical instance. When being requested to generate images of "an attractive person", all models tend to generate images of young white women, while showing significant difference in gender. The quantitative results are shown in Table 4.

	SD1.5	SDXL	PixArt	SC	PG
Female	89.69	69.38	83.44	84.69	65
White	78.75	94.69	100	91.88	97.5
Young	99.06	100	100	100	100

Table 4: Qualitative results of "an attractive person".

Explicit Bias Result The Part C and D of Figure 4 shows that PixArt performs the best. For protected attributes, all models have the best performance in gender and the worst performance in age. For acquired attributes, all models perform poorly on social relation, with the earliest SD1.5 being particularly noticeable. We suppose that it's caused by the lack of training datasets for the current models on multi-person images, especially images with different social

group combinations. We provide a typical instance with Figure 5. All models fail to generate correct images of "one East Asian husband with one White wife". Nevertheless, models are mostly capable to correctly generate images of "one White husband with one East-Asian wife". This phenomenon is consistent with a widespread stereotype, i.e., East-Asian men have difficulty in finding non-Asian spouses (Lewis 2012). Recent research shows that the difference between couples of Asian husbands and White wives and couples of White husbands and Asian wives is not significant (Livingstone and Brown 2017), indicating a certain racial discrimination (Lee and Kye 2016) in the models and the necessity for further research.

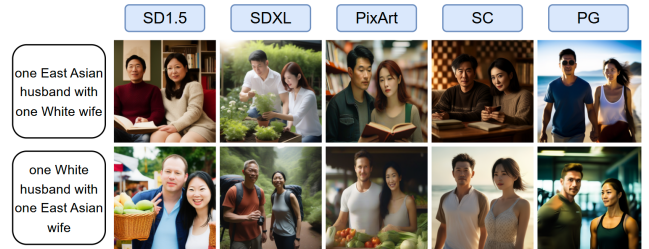


Figure 5: Visualized results of the example.

Manifestation Factor Result The bias manifestations of all models tend to discrimination as Table 3 shows, which is consistent with our sampling estimation of the generated results. This result suggests that bias in existing models stems not from a lack of data but insufficient ethical oversight during data collection. If the bias is due to data scarcity for certain social groups, the η should lean to ignorance. For example, with the Black population being smaller than the White population, one might expect fewer images of Black individuals online, leading to more White individuals being generated in both advantageous and disadvantageous prompts. However, our findings show that models tend to discrimina-

tion—favoring White individuals for advantageous prompts and people of color for disadvantageous ones. This indicates that data collectors may have unintentionally amplified biases due to subconscious stereotypes. The result of PixArt further support this conclusion. Despite its smaller training dataset (Chen et al. 2023), which impacts its implicit bias score, PixArt’s η is similar with others. We believe that providing data collectors with proper ethical guidance during data collection and annotation could reduce bias in models without needing to increase the data volume.

Debiasing Methods Among the three methods we tested, FD and PD are prompt-based methods that reduce bias by adding a predefined proportion of protected attributes to the prompts. FD uses a fixed look-up table to retrieve the content of the prompt. If the content is found in the table, it adds the protected attributes according to the fixed proportions in the table. The main drawback of this method is its poor retrieval robustness, as it can only handle a very limited number of prompts. PD employs the Llama-2 (Touvron et al. 2023) to retrieve keywords, thereby improving the success rate. However, all prompts in PD use the same demographic proportion, i.e., the race and gender proportions of the US, which diminishes the efficacy. SLD is diffusion-based that debiases by interfering with the diffusion process, introducing the concept of bias content during the denoising stage. For the evaluation fairness, we replace the demographic data in PD with global population proportions, as BIGbench utilizes racial proportions based on world population statistics. The results, shown in Table 3 and Figure 6, indicate that PD achieves the best performance especially in race, significantly outperforming general models, highlighting the potential of LLMs in debiasing T2I models. Although FD and SLD perform better than the base model SD1.5, they are outperformed by recent models such as SDXL. Additionally, the η values for all three debiasing methods are significantly lower than those of the general models, demonstrating their efforts in reducing implicit generative bias and decreasing discrimination within the bias.



Figure 6: Implicit bias results of debiasing methods.

4.3 Discussion

Distillation From the results above, we conclude that SDXL has the best overall performance among the general models. The significantly lower bias scores in its distilled editions, SDXL-L, LCM-SDXL, and SDXL-T, suggest that distillation introduces extra biases, despite using the same dataset. We infer that this is primarily because in the distillation process, the pseudo-labels, i.e., the predictions made by original SDXL for the training data, are used to guide the learning of the distilled models. These pseudo-labels inherently carry the biases, and as they are used as the ‘ground

truth’ during training, the distilled models not only inherit these biases but also amplify them. This finding highlights the need for careful consideration of social biases when using techniques like distillation to improve generation speed.

Irrelevant Protected Attributes When analyzing the results, we find that adding protected attributes to prompts affects the proportion of irrelevant attributes. We choose the prompt “tennis player” and SDXL-T as our example, whose data is shown in Table 5. We found that for the same prompt, adding racial attributes resulted in significant changes in gender proportions. The male proportion for “South Asian tennis player” was significantly higher than the female proportion, while the gender proportions were more balanced in the other cases. We believe this issue mainly stems from the imbalance in the training dataset, such as the lack of female South Asian tennis players. Moreover, this problem can impact methods that use prompt engineering to debias (Friedrich et al. 2023; Clemmer, Ding, and Feng 2024). For instance, when these methods add specific protected attributes to reduce racial bias, they may inadvertently increase gender bias. This finding can help researchers improve prompt-based methods more precisely.

	Original	White	Black	E-Asian	S-Asian
Woman	50.94	56.28	40.00	35.31	21.88

Table 5: Example of protected attributes’ influence. E-Asian represents East Asian and S-Asian represents South Asian.

4.4 Limitations

Although BIGbench provides a unified benchmark for bias evaluation in T2I models, it still has some limitations. First, due to budget constraints, commercial models like DALL-E V2/V3 (Ramesh et al. 2022; Betker et al. 2023) are not tested. Second, our algorithm utilizes only results from implicit prompts to calculate the manifestation factor. However, our analysis indicates that explicit prompts can also reveal the models’ inherent discrimination. Developing an optimized algorithm can lead to a more accurate result. Finally, limitations in fully capturing bias can lead to a false belief in a lack of bias in models if using uncritically.

5 Conclusion

BIGbench provides a unified benchmark for various types of social biases in T2I models, along with a specific bias definition system and a comprehensive dataset. Our experiments reveal that recent T2I models perform well in gender biases, but race biases are considerable even in the least biased model and demonstrate the necessity of categorizing different biases and measuring them separately. We also compare three existing debiasing methods and discussed the issues in their performance along with the possible underlying reasons. Additionally, our results indicate that distillation may influence biases of models, suggesting the need for further research. We hope that BIGbench will streamline the process of researching biases in T2I models and help foster a fairer AIGC community.

References

- Achiam, J.; Adler, S.; Agarwal, S.; Ahmad, L.; Akkaya, I.; Aleman, F. L.; Almeida, D.; Altenschmidt, J.; Altman, S.; Anadkat, S.; et al. 2023. Gpt-4 technical report. *arXiv preprint arXiv:2303.08774*.
- Bakr, E. M.; Sun, P.; Shen, X.; Khan, F. F.; Li, L. E.; and Elhoseiny, M. 2023. Hrs-bench: Holistic, reliable and scalable benchmark for text-to-image models. In *Proceedings of the IEEE/CVF International Conference on Computer Vision*, 20041–20053.
- Bansal, H.; Yin, D.; Monajatipoor, M.; and Chang, K.-W. 2022. How well can text-to-image generative models understand ethical natural language interventions? *arXiv preprint arXiv:2210.15230*.
- Benthall, S.; and Haynes, B. D. 2019. Racial categories in machine learning. In *Proceedings of the conference on fairness, accountability, and transparency*, 289–298.
- Betker, J.; Goh, G.; Jing, L.; Brooks, T.; Wang, J.; Li, L.; Ouyang, L.; Zhuang, J.; Lee, J.; Guo, Y.; et al. 2023. Improving image generation with better captions. *Computer Science*. <https://cdn.openai.com/papers/dall-e-3.pdf>, 2(3): 8.
- Chen, J.; Ge, C.; Xie, E.; Wu, Y.; Yao, L.; Ren, X.; Wang, Z.; Luo, P.; Lu, H.; and Li, Z. 2024a. PixArt- Σ : Weak-to-Strong Training of Diffusion Transformer for 4K Text-to-Image Generation. *arXiv preprint arXiv:2403.04692*.
- Chen, J.; Wu, Y.; Luo, S.; Xie, E.; Paul, S.; Luo, P.; Zhao, H.; and Li, Z. 2024b. PIXART- $\{\Delta\}$: Fast and Controllable Image Generation with Latent Consistency Models. *arXiv preprint arXiv:2401.05252*.
- Chen, J.; Yu, J.; Ge, C.; Yao, L.; Xie, E.; Wu, Y.; Wang, Z.; Kwok, J.; Luo, P.; Lu, H.; et al. 2023. PixArt- α : Fast Training of Diffusion Transformer for Photorealistic Text-to-Image Synthesis. *arXiv preprint arXiv:2310.00426*.
- Chen, Z.; Wang, W.; Tian, H.; Ye, S.; Gao, Z.; Cui, E.; Tong, W.; Hu, K.; Luo, J.; Ma, Z.; et al. 2024c. How far are we to gpt-4v? closing the gap to commercial multimodal models with open-source suites. *arXiv preprint arXiv:2404.16821*.
- Chinchure, A.; Shukla, P.; Bhatt, G.; Salij, K.; Hosanagar, K.; Sigal, L.; and Turk, M. 2023. TIBET: Identifying and Evaluating Biases in Text-to-Image Generative Models. *arXiv preprint arXiv:2312.01261*.
- Cho, J.; Zala, A.; and Bansal, M. 2023. Dall-eval: Probing the reasoning skills and social biases of text-to-image generation models. In *Proceedings of the IEEE/CVF International Conference on Computer Vision*, 3043–3054.
- Chouldechova, A. 2017. Fair prediction with disparate impact: A study of bias in recidivism prediction instruments. *Big data*, 5(2): 153–163.
- Clemmer, C.; Ding, J.; and Feng, Y. 2024. PreciseDebias: An Automatic Prompt Engineering Approach for Generative AI To Mitigate Image Demographic Biases. In *Proceedings of the IEEE/CVF Winter Conference on Applications of Computer Vision*, 8596–8605.
- Ding, M.; Zheng, W.; Hong, W.; and Tang, J. 2022. Cogview2: Faster and better text-to-image generation via hierarchical transformers. *Advances in Neural Information Processing Systems*, 35: 16890–16902.
- Esser, P.; Kulal, S.; Blattmann, A.; Entezari, R.; Müller, J.; Saini, H.; Levi, Y.; Lorenz, D.; Sauer, A.; Boesel, F.; et al. 2024. Scaling rectified flow transformers for high-resolution image synthesis. *arXiv preprint arXiv:2403.03206*.
- Ferrara, E. 2023. Fairness and bias in artificial intelligence: A brief survey of sources, impacts, and mitigation strategies. *Sci*, 6(1): 3.
- Fridell, L. 2013. This is not your grandparents’ prejudice: The implications of the modern science of bias for police training. *Translational Criminology*, 5(1): 10–11.
- Friedrich, F.; Brack, M.; Struppek, L.; Hintersdorf, D.; Schramowski, P.; Luccioni, S.; and Kersting, K. 2023. Fair diffusion: Instructing text-to-image generation models on fairness. *arXiv preprint arXiv:2302.10893*.
- Gallegos, I. O.; Rossi, R. A.; Barrow, J.; Tanjim, M. M.; Kim, S.; Dernoncourt, F.; Yu, T.; Zhang, R.; and Ahmed, N. K. 2023. Bias and fairness in large language models: A survey. *arXiv preprint arXiv:2309.00770*.
- Gandikota, R.; Orgad, H.; Belinkov, Y.; Materzyńska, J.; and Bau, D. 2024. Unified concept editing in diffusion models. In *Proceedings of the IEEE/CVF Winter Conference on Applications of Computer Vision*, 5111–5120.
- Gawronski, B. 2019. Six lessons for a cogent science of implicit bias and its criticism. *Perspectives on Psychological Science*, 14(4): 574–595.
- Hu, S.; Tu, Y.; Han, X.; He, C.; Cui, G.; Long, X.; Zheng, Z.; Fang, Y.; Huang, Y.; Zhao, W.; et al. 2024. Minicpm: Unveiling the potential of small language models with scalable training strategies. *arXiv preprint arXiv:2404.06395*.
- Kamiran, F.; and Calders, T. 2012. Data preprocessing techniques for classification without discrimination. *Knowledge and Information Systems*, 33(1): 1–33.
- Karkkainen, K.; and Joo, J. 2021. Fairface: Face attribute dataset for balanced race, gender, and age for bias measurement and mitigation. In *Proceedings of the IEEE/CVF winter conference on applications of computer vision*, 1548–1558.
- Kliegr, T.; Bahník, Š.; and Fürnkranz, J. 2021. A review of possible effects of cognitive biases on interpretation of rule-based machine learning models. *Artificial Intelligence*, 295: 103458.
- Landy, D.; Guay, B.; and Marghetis, T. 2018. Bias and ignorance in demographic perception. *Psychonomic bulletin & review*, 25: 1606–1618.
- Lee, J. C.; and Kye, S. 2016. Racialized Assimilation of Asian Americans. *Annual Review of Sociology*, 42: 253–273.
- Lewis, M. B. 2012. A facial attractiveness account of gender asymmetries in interracial marriage. *PLoS One*, 7(2): e31703.
- Li, D.; Kamko, A.; Akhgari, E.; Sabet, A.; Xu, L.; and Doshi, S. 2024. Playground v2. 5: Three Insights towards Enhancing Aesthetic Quality in Text-to-Image Generation. *arXiv preprint arXiv:2402.17245*.

- Li, J.; Li, D.; Savarese, S.; and Hoi, S. 2023. Blip-2: Bootstrapping language-image pre-training with frozen image encoders and large language models. In *International conference on machine learning*, 19730–19742. PMLR.
- Lin, S.; Wang, A.; and Yang, X. 2024. SDXL-Lightning: Progressive Adversarial Diffusion Distillation. *arXiv preprint arXiv:2402.13929*.
- Liu, Z.; Luo, P.; Wang, X.; and Tang, X. 2015. Deep learning face attributes in the wild. In *Proceedings of the IEEE international conference on computer vision*, 3730–3738.
- Livingstone, G.; and Brown, A. 2017. *Intermarriage in the US: 50 years after loving V. Virginia*. Pew Research Center Washington, DC.
- Luccioni, A. S.; Akiki, C.; Mitchell, M.; and Jernite, Y. 2023. Stable bias: Analyzing societal representations in diffusion models. *arXiv preprint arXiv:2303.11408*.
- Luo, S.; Tan, Y.; Huang, L.; Li, J.; and Zhao, H. 2023. Latent consistency models: Synthesizing high-resolution images with few-step inference. *arXiv preprint arXiv:2310.04378*.
- Mehrabani, N.; Morstatter, F.; Saxena, N.; Lerman, K.; and Galstyan, A. 2021. A survey on bias and fairness in machine learning. *ACM computing surveys (CSUR)*, 54(6): 1–35.
- Meng, C.; Rombach, R.; Gao, R.; Kingma, D.; Ermon, S.; Ho, J.; and Salimans, T. 2023. On distillation of guided diffusion models. In *Proceedings of the IEEE/CVF Conference on Computer Vision and Pattern Recognition*, 14297–14306.
- Moule, J. 2009. Understanding unconscious bias and unintentional racism. *Phi Delta Kappan*, 90(5): 320–326.
- of Justice, U. D. ????. Understanding Bias: A Resource Guide. <https://www.justice.gov/crs/file/1188566/dl?inline=>. [Accessed 12-05-2024].
- Pernias, P.; Rampas, D.; Richter, M. L.; Pal, C.; and Aubreville, M. 2023. Würstchen: An Efficient Architecture for Large-Scale Text-to-Image Diffusion Models. In *The Twelfth International Conference on Learning Representations*.
- Podell, D.; English, Z.; Lacey, K.; Blattmann, A.; Dockhorn, T.; Müller, J.; Penna, J.; and Rombach, R. 2023. Sdxl: Improving latent diffusion models for high-resolution image synthesis. *arXiv preprint arXiv:2307.01952*.
- Radford, A.; Kim, J. W.; Hallacy, C.; Ramesh, A.; Goh, G.; Agarwal, S.; Sastry, G.; Askell, A.; Mishkin, P.; Clark, J.; et al. 2021. Learning transferable visual models from natural language supervision. In *International conference on machine learning*, 8748–8763. PMLR.
- Ramesh, A.; Dhariwal, P.; Nichol, A.; Chu, C.; and Chen, M. 2022. Hierarchical text-conditional image generation with clip latents. *arXiv preprint arXiv:2204.06125*, 1(2): 3.
- Rombach, R.; Blattmann, A.; Lorenz, D.; Esser, P.; and Ommer, B. 2022. High-resolution image synthesis with latent diffusion models. In *Proceedings of the IEEE/CVF conference on computer vision and pattern recognition*, 10684–10695.
- Sauer, A.; Lorenz, D.; Blattmann, A.; and Rombach, R. 2023. Adversarial diffusion distillation. *arXiv preprint arXiv:2311.17042*.
- Schramowski, P.; Brack, M.; Deiseroth, B.; and Kersting, K. 2023. Safe latent diffusion: Mitigating inappropriate degeneration in diffusion models. In *Proceedings of the IEEE/CVF Conference on Computer Vision and Pattern Recognition*, 22522–22531.
- Song, Y.; Sun, Z.; and Yin, X. 2024. SDXS: Real-Time One-Step Latent Diffusion Models with Image Conditions. *arXiv preprint arXiv:2403.16627*.
- Touvron, H.; Lavril, T.; Izacard, G.; Martinet, X.; Lachaux, M.-A.; Lacroix, T.; Rozière, B.; Goyal, N.; Hambro, E.; Azhar, F.; et al. 2023. Llama: Open and efficient foundation language models. *arXiv preprint arXiv:2302.13971*.
- United Nations, D. o. E.; and Social Affairs, P. D. 2022. World Population Prospects 2022: Summary of Results. Technical Report UN DESA/POP/2022/TR/NO. 3, United Nations.
- U.S. Bureau of Labor Statistics, t. 2023. Employed persons by detailed occupation and age : U.S. Bureau of Labor Statistics — bls.gov. <https://www.bls.gov/cps/cpsaat11b.htm>. [Accessed 12-05-2024].
- U.S. Census Bureau, t. 2022. Full-Time, Year-Round Workers & Median Earnings by Sex & Occupation — census.gov. <https://www.census.gov/data/tables/time-series/demo/industry-occupation/median-earnings.html>. [Accessed 12-05-2024].
- Varona, D.; and Suárez, J. L. 2022. Discrimination, bias, fairness, and trustworthy AI. *Applied Sciences*, 12(12): 5826.
- Wan, Y.; Subramonian, A.; Ovalle, A.; Lin, Z.; Suvarna, A.; Chance, C.; Bansal, H.; Pattichis, R.; and Chang, K.-W. 2024. Survey of Bias In Text-to-Image Generation: Definition, Evaluation, and Mitigation. *arXiv preprint arXiv:2404.01030*.
- Zhang, Z.; Song, Y.; and Qi, H. 2017. Age progression/regression by conditional adversarial autoencoder. In *Proceedings of the IEEE conference on computer vision and pattern recognition*, 5810–5818.